THE PUBLISHING HOUSE
OF THE ROMANIAN ACADEMY

PROCEEDINGS OF THE ROMANIAN ACADEMY, Series A,
Volume10 , Number 3/2009 , pp.000-000

ON THE SHAPE RECONSTRUCTION OF 3D STOKES FLOWS

Dinel POPA [1], Eliza MUNTEANU [2], Ligia MUNTEANU [3], Veturia CHIROIU [3]

[1] University of Piteşti, dept of Applied Mechanics, Târgul din Vale 1, 110040 Piteşti
[2] National Institute for Aerospace Research "Elie Carafoli", Bd. Iuliu Maniu 220, 061126 Bucharest
[3] Institute of Solid Mechanics, Romanian Academy, Ctin Mille 15, 010141 Bucharest
Corresponding author: Veturia CHIROIU, E-mail: veturiachiroiu@yahoo.com

This paper deals with the ill-posed nonlinear problem of the shape reconstruction of the Stokes fluid flow. Shape parameters are estimated with a genetic algorithm inverse method by reducing the errors (objective function) between estimated and observed velocity-pressure data. Recommendation concerning the proposed technique is deduced with regard to the algorithm performance

Key Words: Shape reconstruction, Stokes flow, Genetic algorithm.

1. INTRODUCTION

There are few studies in the literature considering the shape reconstruction of an immersed obstacle using the genetic algorithms. A theoretical foundation of the shape reconstruction of 3D Stokes flows is given by Yan and Ma [1] by establishing the differentiability of the initial boundary value problem with respect to the interior boundary curve in the sense of a domain derivative. These authors solved the problem by a regularized Newton method. They established the domain derivative of the Stokes equations in a multiple bounded domain, and derived an efficient numerical approach for the solution of the 2D realizations of such problem. In [2], Yan and Ma solved a shape reconstruction problem for heat conduction with mixed condition, and, in [3], the same authors derived the expressions of domain derivative for the steady Navier–Stokes equations

Chapko, Kress and Yoon [4], [5] consider the inverse boundary problem for the time-dependent heat equation in the case of perfectly conducting and insulating inclusions. Hettlich [6] and Kirsch [7] solved the inverse obstacle scattering problem for sound soft and sound hard obstacles. Other publications on closely related topics are revealed by Matsumoto and Kawahara [8], Newman III *et al*. [9], Katamine *et al.* [10], Bernad *et al.* [11], Carabineanu [12], Dumitrescu, Cardoş and Alexandrescu [13]. The problem addressed by this paper is the shape reconstruction of 3D flows governed by Stokes equations from pressure-velocity data by using a genetic algorithm GA. Genetic algorithms are a class of optimization algorithms that mimic genetic recombination and natural selection (Goldberg [14], Giuclea *et al.*[15], Preda [16]).

To our knowledge, the shape reconstruction of the Stokes fluid flow has not yet been solved by using a genetic algorithm. In our case, the GA is based on the modeling of the unknown boundary as a *n*-ellipsoid with only 10 parameters (Bonnet [17], Chiroiu, Munteanu and Nicolescu [18]). This paper deals with the shape reconstruction of the Stokes fluid flow. Shape parameters are estimated with a genetic algorithm inverse method.

2. FORMULATION OF THE PROBLEM

The aim of the problem is to find the velocity of the fluid $u=(u_1,u_2,u_3)$ and the pressure p, defined in $\Omega=\Omega_1\setminus\Omega_2$, $\bar{\Omega}_2\subset\Omega_1$, with Ω_1 and Ω_2 two simply connected bounded domains of class C^2 in R^3. The

boundaries of Ω_1 and Ω_2 are denoted by Γ_1 and Γ_2, respectively. The fields u and p satisfy the following equations and boundary condition

$$-\mu\Delta u+\nabla p=f \text{ in } \Omega,\ \operatorname{div}u=0 \text{ in } \Omega,\ u=0 \text{ on } \Gamma_1,\ u=0 \text{ on } \Gamma_2, \tag{2.1}$$

where f is an applied body force in Ω, and μ the coefficient of kinematic viscosity. The Reynolds number is defined as the inverse of μ, i.e. $\mathrm{Re}=1/\mu$. The divergence free condition $\operatorname{div}u=0$ in Ω comes from the fact that the fluid has a homogeneous density and evolves as an incompressible flow. The shape of Ω_2, i.e. the interior boundary Γ_2 is unknown, and the solution u and respectively the pressure p of (2.1) depend on Γ_2 : $u=u_{\Gamma_2}$, $p=p_{\Gamma_2}$. Both, the divergence free condition and the unknown surface Γ_2 conditions are difficult to impose on the mathematical and numerical point of view. To solve the problem (2.1) an optimization technique is applied using a genetic algorithm (Deb [19], Chiroiu and Munteanu [20], Chiroiu *et al*. [21], [22]).

3. DESCRIPTION OF UNKNOWN GEOMETRY OF Γ_2

The model considered here is to determine the unknown interior boundary Γ_2 by using an *n*-ellipsoid [17], [18]. The goal of the inverse problem is to find the set of parameters (shape parameters) that define Γ_2 such that the *n*-ellipsoid best fits the set of data points. An *n*-ellipsoid is defined by 10 shape parameters d_i, $i=1,2,...10$: arbitrary center coordinates x_G, y_G, z_G, principal axes a,b,c, the principal directions defined by Euler angles ξ,ψ,ζ and the exponent n. The advantage of this model is the small number of parameters needed to represent a shape. The boundary Γ_2 is defined as the image of the unit *n*-sphere S of equation

$$x^n+y^n+z^n=1, \tag{3.1}$$

through the affine transformation

$$y=(Y_1,Y_2,Y_3)\in S \rightarrow\ y=(y_1,y_2,y_3)\in\Gamma_2, \tag{3.2}$$

with

$$\begin{gathered} y_1=x_G+r_{11}aY_1+r_{12}bY_2+r_{13}cY_3,\ \ y_2=y_G+r_{21}aY_1+r_{22}bY_2+r_{23}cY_3, \\ y_3=z_G+r_{31}aY_1+r_{32}bY_2+r_{33}cY_3, \end{gathered} \tag{3.3}$$

where $r_{ij}=r_{ij}(\xi,\psi,\zeta)$ are the components of the rotation, which transforms the coordinate axes into the principal axes of the ellipsoid. These components are given by

$$R(z,\psi)=\begin{bmatrix}\cos\psi & -\sin\psi & 0\\ \sin\psi & \cos\psi & 0\\ 0 & 0 & 1\end{bmatrix},\ R(x,\xi)=\begin{bmatrix}1 & 0 & 0\\ 0 & \cos\xi & -\sin\xi\\ 0 & \sin\xi & \cos\xi\end{bmatrix},\ R(z,\xi)=\begin{bmatrix}\cos\zeta & -\sin\zeta & 0\\ \sin\zeta & \cos\zeta & 0\\ 0 & 0 & 1\end{bmatrix}. \tag{3.4}$$

For $n=2$, (3.1) yields the usual unit sphere and for $n=\infty$ the unit cube of vertices $(\pm1,\pm1,\pm1)$. By using (3.2) and (3.3) the unit sphere and the unit cube are respectively transformed into ellipsoids and boxes, with arbitrary center, size and orientation. The continuous dependence of the solutions u and p on variations of the unknown boundary Γ_2 was established in [1]. Extra data is necessary in order to solve the inverse problem, i.e. the velocity u and the pressure p measured on a surface S_0 exterior to Γ_2.

3. MINIMIZATION ALGORITHM

The minimization algorithm is formulated as :
Given u *and* p *on a surface* S_0 *exterior to* Γ_2

$$u|_{S_0} \equiv \hat{u}\ ,\ \ p|_{S_0} \equiv \hat{p}\ , \tag{4.1}$$

(1) *find* Γ_2 *as the minimizer of the distance* $I(\Gamma_2)$ *between the measure data* $\hat{u}$ *and* $\hat{p}$ *and computed data* u_{Γ_2} *and* p_{Γ_2} *for a fixed location of* Γ_2

$$\min_{\Gamma_2} I(\Gamma_2)\ ,\ I(\Gamma_2) \equiv I(u_{\Gamma_2}, p_{\Gamma_2})\ , \tag{4.2}$$

(2) find u and p in $\Omega = \Omega_1 \setminus \Omega_2$, subject to constraints

$$g_1(u,p,\Gamma_2) = \mu\Delta u - \nabla p + f = 0 \ \text{ in } \Omega\ ,$$

$$g_2(u,p,\Gamma_2) = \operatorname{div} u = 0 \ \text{ in } \Omega\ , \tag{4.3}$$

$$g_3(u,p,\Gamma_2) = u = 0 \ \text{ on } \Gamma_1\ ,\ g_4(u,p,\Gamma_2) = u = 0 \ \text{ on } \Gamma_2\ ,$$

in conforming with (2.1). Here, the boundary Γ_2 is sought by determining 10 shape parameters d_i, $i = 1,2,...10$, from minimizing the distance $I(\Gamma_2)$ between the measured and computed data on S_0.

The least-squares functional is defined as

$$I(\Gamma_2) = \frac{1}{2}\int_{S_0} \left(|u(y) - \hat{u}(y)|^2 + |p(y) - \hat{p}(y)|^2 \right) dS_y\ . \tag{4.4}$$

To avoid the computation of the derivatives of (4.4) with respect to Γ_2, the functional (4.4) is replaced by

$$J(\Gamma_2) = \frac{1}{2}\sum_{i=1}^{m} |u_i - \hat{u}_i|^2 + |p_i - \hat{p}_i|^2\ , \tag{4.5}$$

where m is the number of observed points on S_0. For each solution u and p in $\Omega = \Omega_1 \setminus \Omega_2$, and boundary Γ_2, the constraint violation for each constraint (4.3) is calculated as follows [19]

$$\omega_i(u,p,\Gamma_2) = \begin{cases} |g_i(u,p,\Gamma_2)|, & \text{if } g_i(u,p,\Gamma_2) \neq 0, \\ 0, & \text{if otherwise,} \end{cases} \quad i = 1,2,3,4. \tag{4.6}$$

Thereafter, all constraints violations are added together to get the overall constraint violation.

$$J(u,p,\Gamma_2) = \frac{1}{2}\sum_{i=1}^{m} |u_i - \hat{u}_i|^2 + |p_i - \hat{p}_i|^2 + \sum_{i=1}^{4} \omega_i(u,p,\Gamma_2)\ . \tag{4.7}$$

By taking account of (4.7), the minimization algorithm (4.1)-(4.4), can be formulated as :
Given u *and* p *on a surface* S_0 *exterior to* Γ_2

$$u|_{S_0} \equiv \hat{u}\ ,\ \ p|_{S_0} \equiv \hat{p}\ , \tag{4.8}$$

find Γ_2, u *and* p *in* $\Omega = \Omega_1 \setminus \Omega_2$ *from*

$$\min_{\Gamma_2} J(u,p,\Gamma_2) = \frac{1}{2}\sum_{i=1}^{m} |u_i - \hat{u}_i|^2 + |p_i - \hat{p}_i|^2 + \sum_{i=1}^{4} \omega_i(u,p,\Gamma_2)\ . \tag{4.9}$$

Nonlinear minimization problem (4.8) and (4.9) is numerically solved by using a genetic algorithm. The numerical implementation requires the forward solution of (2.1) for reasonable a priori information for observed data u and p on a surface S_0 exterior to Γ_2 (4.1). The forward solution is solved by FEM.

5. SIMULATION STUDIES AND RESULTS

As the same *n*-ellipsoid can result from many combinations of Euler angles and permutations of principal axes, it is difficult to measure the accuracy of the identification of Γ_2 by means of comparison of the identified parameters d_i, $i=1,2,...,10$ with those defining the true Γ_2 and used to compute the simulated data. Instead, the relative errors $\varepsilon_V, \varepsilon_A, \varepsilon_I$ for the volume, boundary area and geometrical inertia tensor (with respect to the fixed coordinates $Ox_1x_2x_3$) are computed. The indicator ε_I is very sensitive to the orientation of Γ_2 in space, together with the ratios J_n / J_0, where $J_n = J(u, p, \Gamma_n)$ and J_0 an initial value. Γ_n is the current Γ_2 after the *n*-th iteration of the minimization process. Expressions of indicators $\varepsilon_V, \varepsilon_A, \varepsilon_I$ in terms of boundary integrals are as follows [17]

$$\varepsilon_V = \frac{V(\Gamma_n)}{V(\Gamma_2)} - 1,\ V(S_0) = \frac{1}{3}\int_S y_i n_i \mathrm{d}S_y,\quad \varepsilon_A = \frac{A(\Gamma_n)}{A(\Gamma_2)} - 1,\ A(S_0) = \int_S \mathrm{d}S_y, \tag{5.1}$$

$$\varepsilon_I = \left(\frac{\sum_{1\le i,j\le 3} (I_{ij}(\Gamma_n) - I_{ij}(\Gamma_2))^2}{\sum_{1\le i,j\le 3} I_{ij}^2(\Gamma_2)} \right)^{1/2},\ I_{ij}(S) = \frac{1}{5}\int_S y_i y_j y_k n_k \mathrm{d}S_y, \tag{5.2}$$

where S is the unit *n*-sphere defined by (3.1).

The genetic algorithm starts with an initial population of $N_{pop} = 10$ chromosomes which is a $N_{pop} \times N_{bits}$ matrix filled with randomly generated ones and zeros bits. Natural selection occurs each generation or iteration of the algorithm. Every iteration, $N_{good} = 0.5 N_{pop}$ chromosomes are used for reproducing while the discarded chromosomes N_{bad} are replaced by new offspring. The approach uses the single-point crossover where a crossover point is randomly selected. Mutation points are randomly selected from $N_{pop} \times N_{bits}$ bits in the population matrix.

Table 5.1 Results for non-perturbed data ($\varepsilon = 0$) for reconstruction of Γ_2.

Ω_2	α	Iterations	$J_{final} / J_0 \times 10^{-7}$	$\varepsilon_V \times 10^{-7}$	$\varepsilon_A \times 10^{-6}$	$\varepsilon_I \times 10^{-5}$
sphere	0.01	63	3.88	8.22	6.13	9.54
	0.15	72	3.61	7.56	5.34	8.02
	0.24	75	2.29	7.14	5.41	8.05
	0.50	80	3.53	8.67	5.47	9.91
	0.75	94	3.75	8.99	6.09	9.33
Rectangular box	0.01	68	3.59	11.40	10.22	9.13
	0.15	69	3.17	10.66	8.25	8.75
	0.24	59	2.14	8.78	7.45	7.34
	0.50	82	2.99	9.15	7.78	7.83
	0.75	89	3.18	9.33	6.90	8.33

The number of mutation is given by relation $N_{mutations} = \alpha N_{pop} N_{bits}$, where $0 < \alpha < 1$ is the mutation rate (Majdalani, Angulo-Jaramillo and Di Piedro [23]). Mutations are not allowed on the final iteration and on a number N_{elite} of the best solution (elite solution) that propagate unchanged. The algorithm is run for a number of generations $N_{generations} = 100$ and N_{elite}=1. The starting population is the same for different α

values. In our numerical examples, the exterior domain Ω_1 is a sphere of radius 1. Two geometries are taken for interior domain Ω_2, i.e. a sphere with radius 0.16 ($m = 50$ points) and a rectangular box of dimensions (0.28, 0.21, 0.02) ($m = 65$ points). The number of iterations of genetic algorithm, the values of J_{final} / J_0, $\varepsilon_V, \varepsilon_A, \varepsilon_I$ for different values of α and the Reynolds number $\mathrm{Re} = 100$, are displayed in table 5.1, in the case of non-perturbed data.

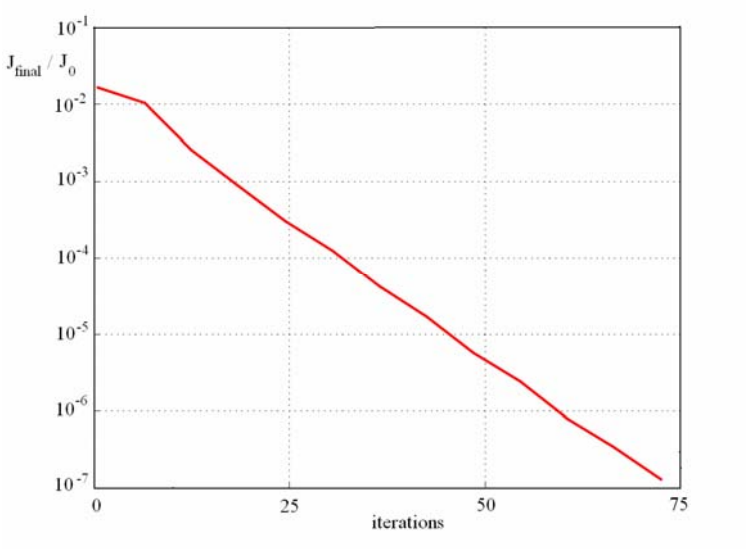

Fig.5.1. Convergence history of J_{final} / J_0 for sphere.

We see from this table that for all domains the accuracy is acceptable for $\alpha = 0.24$. Numerical experiments show that the value of J_{final} / J_0 reaches a maximum for $\alpha = 0.01$ and a minimum for $\alpha = 0.24$. The increase of α beyond 0.24 decreases the performance of the algorithm. The error indicators $\varepsilon_V, \varepsilon_A, \varepsilon_I$ reach a maximum for $\alpha = 0.01$ and a minimum for $\alpha = 0.24$ for all domains.

The convergence history of J_{final} / J_0, for $\alpha = 0.24$, are displayed in fig. 5.1 for the sphere, and in fig. 5.2 for the rectangular box, respectively.

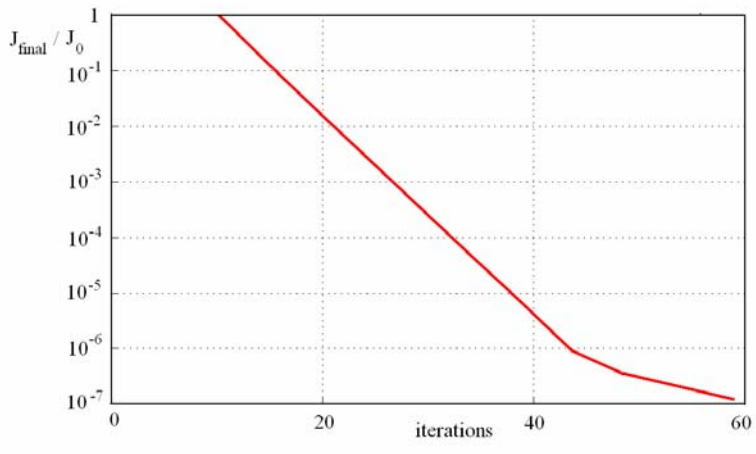

Fig.5.2. Convergence history of J_{final} / J_0 for rectangular box.

Results for perturbed data ($\varepsilon = 10^{-3}$) are shown in table 5.2. For all cases, J_{final} / J_0 reaches a maximum for $\alpha = 0.01$ and a minimum for $\alpha = 0.24$. We see that the numerical solution of the inverse problem hence behaves well with respect to perturbed data. This is probably a consequence of the fact that unknown

geometry is described using only 10 parameters. This behavior was also observed for different initial populations and different values of N_{elite}. For N_{elite}=0 and N_{elite}=2, the numerical solution becomes instable with respect to measurement noise and the convergence is reached after a very large number of iterations, with a lower accuracy. For N_{elite}=1, all cases exhibit very good convergence and accuracy, especially for non-perturbed data. Fig.5.3 displays the initial, exact and approximate shapes of both interior domains for randomly different centers.

Table 5.2 Results for perturbed data ($\varepsilon = 10^{-3}$).

Ω_2	α	Iterations	$J_{final}/J_0 \times 10^{-6}$	$\varepsilon_V \times 10^{-6}$	$\varepsilon_A \times 10^{-5}$	$\varepsilon_I \times 10^{-4}$
sphere	0.01	69	2.34 %	2.95	3.78	3.33
	0.15	71	2.32 %	2.81	2.44	3.21
	0.24	73	1.44 %	2.45	3.87	2.48
	0.50	85	1.66%	2.97	4.20	4.45
	0.75	99	1.77%	3.10	4.41	4.62
Rectangular box	0.01	101	1.45	3.45	2.54	2.93
	0.15	109	1.38	2.68	1.65	2.33
	0.24	109	0.38	2.08	0.98	1.56
	0.50	123	1.19	2.19	1.39	2.78
	0.75	119	1.37	3.03	2.19	3.23

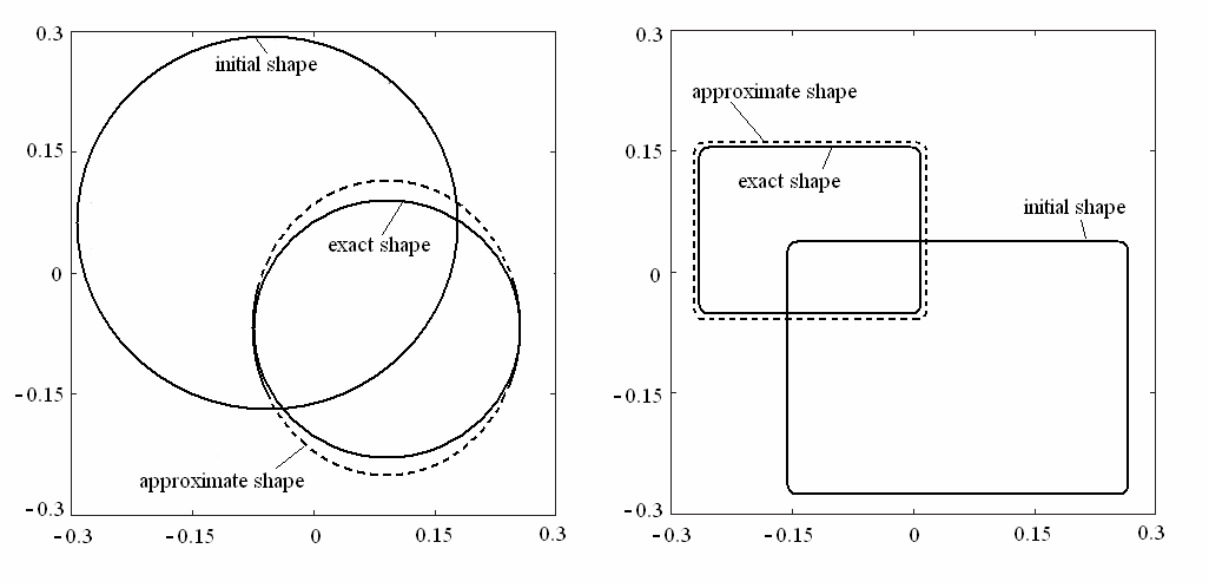

Fig.5.3. Interior domains Ω_2 with initial, exact and approximate boundaries, for randomly different centers.

6. CONCLUSIONS

The conclusions of the article are as follows: We determine the unknown interior boundary Γ_2 by using an *n*-ellipsoid. This allows finding the shape parameters such that the *n*-ellipsoid best fits the set of data points. The results of several numerical experiments show that GA gives good reconstruction, and indicate the feasibility of the algorithm. The basic components of the inversion strategy perform well when a moderate number of shape parameters are used for the description of the unknown domain.

Several mutation rates and numbers of elite solutions were explored in order to study their influence on the algorithm fitness. It was found that the mutation rate α is a sensitive parameter which has an optimum value around 0.24 yielding best performance. A good elitist strategy is obtained only for N_{elite}=1. The results obtained on the model problem show the efficiency of GA for the shape reconstruction of the Stokes fluid flow. The GA can find the optimal solution in one single simulation run due to their population-approach.

We conclude that the proposed algorithm is a basic tool in the design of many industrial devices such as aircraft wings, automobile shapes, boats, and so on.

ACKNOWLEDGEMENT.

The authors gratefully acknowledge the financial support of the National Authority for Scientific Research (ANCS, UEFISCSU), Romania, through PN-II research project code ID_1391/2008.

REFERENCES

1. YAN, W.-J., MA, Y.-C., *Shape reconstruction of an inverse Stokes problem*, J. Computat. Appl. Math., Vol. 216, pp.554 – 562, 2008.
2. YAN, W.-J., MA, Y.-C., *The application of domain derivative for heat conduction with mixed condition in shape reconstruction*, Appl. Math. Computat., Vol.181, nr.2, pp.894–902, 2006.
3. YAN, W-J., MA, Y.-C., *A numerical method for the reconstruction of a cavity*, J. Computat. Appl. Math., under review.
4. CHAPKO, R., KRESS, R., YOON, J.-R., *On the numerical solution of an inverse boundary value problem for the heat equation*, Inverse Problems, Vol.14, pp.853–867, 1998.
5. CHAPKO, R., KRESS, R., YOON, J.-R., *An inverse boundary value problem for the heat equation: the Neumann condition*, Inverse Problems, Vol.15, pp.1033–1046, 1999.
6. HETTLICH, F., *Frechet derivatives in inverse obstacle scattering*, Inverse Problems, Vol.11, pp.371–382, 1995.
7. KIRSCH, A., *The domain derivative and two applications in inverse scattering theory*, Inverse Problems, Vol. 9, pp.81–96, 1993.
8. MATSUMOTO, J.; KAWAHARA, M., *Shape identification for fluid-structure interaction problem using improved bubble element*, Int. J. of Computational Fluid Dynamics, Vol. 15, issue 1, pp. 33–45,2001.
9. NEWMAN III, J.C., TAYLOR III, A.C., BARNWELL, R.W., NEWMAN, P.A., HOU, G. J.-W. , *Overview of sensitivity analysis and shape optimization for complex aerodynamic configurations*, Journal of Aircraft, Vol.36, pp. 87–96, 1999.
10. KATAMINE, E., AZEGAMI, H., TSUBATA, T., ITOH, S., Solution *to shape optimization problems of viscous flow fields*, Int. J. of Computational Fluid Dynamics, Vol. 19 pp. 45–51, 2005.
11. BERNAD, S., SUSAN-RESIGA, R., MUNTEAN, S., ANTON, I., Numerical analysis of the cavitating flows, Proc. of the Romanian Academy, Series A: Mathematics, Physics, Technical Sciences, Information Science, Vol. 7, nr.1, 2006.
12. CARABINEANU, A., *Supersonic flow past a grid of thin profiles*, Proc. of the Romanian Academy, Series A: Mathematics, Physics, Technical Sciences, Information Science, Vol.4, nr.2, pp.83 –92, 2003.
13. DUMITRESCU, H., CARDOŞ, V., ALEXANDRESCU, N., *Computation of separating laminar boundary-layer flows*, Proc. of the Romanian Academy, Series A: Mathematics, Physics, Technical Sciences, Information Science, Vol. 4, nr.3, pp. 151–156, 2003.
14. GOLDBERG, D.E., *The design of innovation: Lessons from Genetic Algorithms, lessons for the real world,* Technological Forecasting and Social Change, Vol.64, pp.7–12, 2000.
15. GIUCLEA, M., SIRETEANU, T., STĂNCIOIU, D., STAMMERS, C.W., *Modelling of magnetorheological damper dynamic behavior by genetic algorithms based inverse method*, Proc. of the Romanian Academy, Series A: Mathematics, Physics, Technical Sciences, Information Science, Vol. 5, nr.1, 2004.
16. PREDA, V., Nondifferentiable mathematical programs. Optimality and higher=order duality results, Proc. of the Romanian Academy, Series A: Mathematics, Physics, Technical Sciences, Information Science, Vol. 9, nr.3, 2008.
17. BONNET, M., *Shape identification problems using boundary elements and shape differentiation*, Proc. of the 2-nd National Conf. on Boundary and Finite Element, ELFIN2, Sibiu, pp. 35–48, 1993.
18. CHIROIU, V., MUNTEANU, L., NICOLESCU, C.M., *Shape description of general 3D object using tactile sensing information*, AMSE: Advances in Modelling, Series B: Signal Processing and Pattern Recognition, Vol.47, nr.3, pp.81–90, 2004.
19. DEB, K., *Multi-objective optimization using evolutionary algorithms*, John Wiley & Sons, LTD, 2004.
20. CHIROIU, V., MUNTEANU, L., *Estimation of micropolar elastic moduli by inversion of vibrational data*, Complexity International Journal, Vol.9, pp.16–25, 2002.
21. CHIROIU, V., MOLDOVEANU, F., CHIROIU, C., SCALERANDI, M., RUFFINO, E., *Application of genetic algorithm in defects visualization*, Roum. des Sci. Techn., tome 44, nr. 3, 1999.
22. CHIROIU, C., MUNTEANU, L., CHIROIU, V., DELSANTO, P.P., SCALERANDI, M., *A genetic algorithm for determining of the elastic constants of a monoclinic crystal*, Inverse Problems, Vol.16, pp.121–132, 2000.
23. MAJDALANI, S., ANGULO-JARAMILLO, R., DI PETRO L., *Estimating preferential water flow parameters using a binary genetic algorithm inverse method*, Environmental Modelling & Software, Vol.23, pp.950–956, 2008.

Received January 27, 2009